

PAPER

# Effects of delayed Kerr nonlinearity on the propagation of femtosecond annular Gaussian filaments in air

To cite this article: Junping Lan *et al* 2019 *Phys. Scr.* **94** 105225

View the [article online](#) for updates and enhancements.

## You may also like

- [Millimeter Light Curves of Sagittarius A\\* Observed during the 2017 Event Horizon Telescope Campaign](#)  
Maciek Wielgus, Nicola Marchili, Iván Martí-Vidal et al.
- [A Universal Power-law Prescription for Variability from Synthetic Images of Black Hole Accretion Flows](#)  
Boris Georgiev, Dominic W. Pesce, Avery E. Broderick et al.
- [Broadband Multi-wavelength Properties of M87 during the 2017 Event Horizon Telescope Campaign](#)  
The EHT MWL Science Working Group, J. C. Algaba, J. Anzarski et al.

# Effects of delayed Kerr nonlinearity on the propagation of femtosecond annular Gaussian filaments in air

Junping Lan<sup>1</sup> , Chengxin Yu<sup>2</sup>, Yuan Liu<sup>1</sup> , Zhifang Feng<sup>1,5</sup> , Libin Fu<sup>3,4,5</sup> and Jie Liu<sup>2,4</sup>

<sup>1</sup> College of Applied Science, Taiyuan University of Science and Technology, Taiyuan 030024, People's Republic of China

<sup>2</sup> Institute of Applied Physics and Computational Mathematics, Beijing 100088, People's Republic of China

<sup>3</sup> Graduate School, China Academy of Engineering Physics, Beijing 100193, People's Republic of China

<sup>4</sup> HEDPS, CAPT, and CICIFSA MoE, Peking University, Beijing 100871, People's Republic of China

E-mail: [fengzf@tyust.edu.cn](mailto:fengzf@tyust.edu.cn) and [lbfu@gscaep.ac.cn](mailto:lbfu@gscaep.ac.cn)

Received 1 February 2019, revised 24 June 2019

Accepted for publication 2 July 2019

Published 13 August 2019



CrossMark

## Abstract

The effects of the delayed Kerr nonlinearity on the annular Gaussian filaments nearby the characteristic time of the molecular rotational respond are numerically investigated. The simulated results show that the delayed Kerr nonlinearity leads to the advancement of the filament onset distance when the pulse duration is fixed. Moreover, in the presence of the delayed Kerr nonlinearity, the length of the filament is obviously extended, and the peak plasma density appears the great oscillations that makes the filament become unstable and nonuniform. These results are mainly induced by the redistribution of the fluence and the modulation of the speed of the total energy loss in the presence of the delayed Kerr nonlinearity. Moreover, the delayed Kerr nonlinearity enhances the self-focusing of the trailing edge and leads further to the extension of the optical filament. This research is of great significance to deeply understand the long-distance transmission characteristics of the annular Gaussian filaments.

Keywords: filamentation, the delayed Kerr nonlinearity, femtosecond annular Gaussian beam

(Some figures may appear in colour only in the online journal)

## 1. Introduction

Femtosecond laser filamentation, resulting from the dynamic balance between the Kerr self-focusing due to a nonlinear intensity-dependent refractive index and the defocusing on laser induced plasma, has been the subject of active research in strong-field science [1]. During the propagation of optical filament, it not only presents many exciting properties [2–4], but have also attracted much attention for their various important applications. For instance, the recognition of distant targets by laser-induced breakdown spectroscopy [5, 6], lightning control [7–9] and remote sensing of atmospheric pollutants [10–12], etc. Particularly, in recent years, one of the considerably interesting aspects is the adoption of some

nonconventional beam shapes in optical filamentation, such as hollow Gaussian beams [13, 14], ring-Airy beams [15], Bessel beams [16, 17] as well as annular Gaussian beams [18–20]. Due to their potential applications in the fields of plasma, atomics, and modern optics [21–23], exploring the fundamental characteristics processes of these non-Gaussian filaments (annular Gaussian filament in this paper) is extremely essential.

The propagation of intense femtosecond laser pulses in air involves varieties of linear and nonlinear optical processes, such as diffraction, nonlinear Kerr self-focusing, ionization and plasma defocusing. These processes play a significant role in the propagation dynamics of the laser pulse. For the nonlinear Kerr self-focusing, except that the instantaneous Kerr nonlinearity on account of the electronic response can influence laser beam propagation, the delayed Kerr nonlinearity because of nuclear

<sup>5</sup> Authors to whom any correspondence should be addressed.

rotational response also plays a significant role in the propagation of high power femtosecond laser filaments in air. In early years, several groups showed that the delayed response mainly changed the nonlinear refractive index and further led to the spectral change [24, 25]. Milchberg *et al* also firstly observed the strong effect of quantum rotational wave packets in air during the long-range filamentary propagation [26]. In addition, the delayed Kerr nonlinearity not only strongly modifies the dynamics of propagation by distorting the pulse shape [27, 28], but also dramatically changes the beam diameter, the beam time-splitting, the on-axis laser intensity and the electron density [29]. However, when the pulse duration is far from the characteristic time ( $\tau_\kappa = 70$  fs) of the molecular rotational response in air, the delayed Kerr nonlinearity could be neglected in the propagation of optical filament in air [30–33]. At present, it remains unclear that the delayed Kerr nonlinearity depends on the different initial pulse lengths near the characteristic time.

In this paper, we have primarily analyzed the effects of the delayed Kerr nonlinearity on the optical filament produced by an annular Gaussian beam (the beam with zero center intensity). In our previous work [32], we proposed a new scheme that an annular Gaussian beam and a conventional Gaussian beam passed through an optical system, which was composed of an axicon and a plano-concave lens, and analyzed specifically the difference of the modulation effect of the concave lens and the nonlinear dynamics mechanism between the two types of laser beams. The results demonstrated that the combination of an axicon with a concave lens can increase the length of the ring-Gaussian filament remarkably comparing with Gaussian filament under the same initial condition. Furthermore, the extension effect of the concave lens on filament was more sensitive to the ring-Gaussian beam than the Gaussian beam. Therefore, this complicated focusing geometry, which in fact had been proposed by the group of Tzortzakis [34], was more favorable for ring-Gaussian beam to produce a long distance filamentation, and the ultrashort ring-Gaussian beam perhaps offered a new and an efficient route towards the generation of extended optical filament. However, the delayed response by reason of the short pulse duration ( $\tau_0 = 40$  fs) was ignored. Thus, it is necessary to explore how the delayed Kerr nonlinearity affects the propagation of the annular Gaussian filament near the characteristic time of the molecular rotational response.

## 2. Model and propagation equations

In this work, we still use our previously proposed model [32, 33]. A femtosecond annular Gaussian beam at central wavelength  $\lambda_0 = 800$  nm with a larger diameter (denoted by the radius  $r_0$ ) wavefront passes through an optical system, which is composed of a shallow axicon and a fused silica plano-concave lens. The axicon lens incurs a linear spatial chirp,  $C \approx k_0(n - n_0)\alpha$  is related to the shallow angle of the axicon,  $\alpha$ , to the annular wave ( $\propto e^{-iCr}$ ) in the transverse plane, where  $n_0$  and  $n$  are the refractive index of the air and the glass axicon, respectively, and  $r$  is the transverse radial coordinate. The introduction of a diverging lens actually leads

to an effective base angle of lens,  $\alpha_{\text{eff}} = \alpha + r/[(n - n_0)f]$ , where  $f$  is the focal distance of the concave. The corresponding effective phase chirp coefficient is  $C_{\text{eff}}$ , which makes the annular wave in the transverse plane be proportional to  $\exp(-iC_{\text{eff}}r)$ . Thus, the incident pulse can be written as:

$$A(r, t, z = 0) = A_0 \exp \left[ -\frac{(r - r_0)^2}{w_0^2} - \frac{t^2}{\tau_0^2} \right] \times \exp(-iC_{\text{eff}}r), \quad (1)$$

where  $A_0$ ,  $w_0$  and  $\tau_0$  are the initial electric field amplitude,  $e^{-2}$  beam waist, and the pulse duration, respectively.

The propagation dynamics of a femtosecond pulse in air can be simulated numerically through the linearly polarized laser electric field  $A(r, t, z)$  with cylindrical symmetry around the propagation axis  $z$ , which bases on an extended nonlinear Schrödinger equation coupled with the laser-plasma production due to multiphoton ionization mechanism. In the moving reference frame with the group velocity  $v_g = c$  ( $c$  is the light speed in vacuum) and the slowly varying envelope approximation, the coupled equations can be written as [27, 28]

$$\frac{\partial A}{\partial z} = \frac{i}{2k_0} \nabla_{\perp}^2 A - i \frac{\beta_2}{2} \frac{\partial^2 A}{\partial t^2} + ik_0 N_{\text{Kerr}} A - ik_0 \frac{n_e}{2n_c} A - \frac{\beta^{(K)}}{2} |A|^{2K-2} A, \quad (2)$$

$$N_{\text{Kerr}} = \frac{n_2}{2} \left( |A|^2 + \frac{1}{\tau_\kappa} \int_{-\infty}^t |A|^2 dt' \right) \times \exp \left[ -\frac{(t - t')}{\tau_\kappa} \right] |A(t')|^2 dt', \quad (3)$$

$$\frac{\partial n_e}{\partial t} = \frac{\beta^{(K)}}{K\hbar\omega_0} |A|^{2K} \left( 1 - \frac{n_e}{n_{\text{at}}} \right), \quad (4)$$

where  $\nabla_{\perp}^2$  describes the beam transverse diffraction, and  $k_0 = 2\pi/\lambda_0$  ( $\lambda_0 = 800$  nm) is the central wave number. The second term on the right-hand side of equation (2) describes the group velocity dispersion with the coefficient  $\beta_2 = 0.2$  fs<sup>2</sup> cm<sup>-1</sup>. The third term,  $N_{\text{Kerr}}$ , results from the intensity-dependent refractive index and includes both instantaneous and retarded contributions. The nonlinear index of refraction and the characteristic time of the Raman response are  $n_2 = 3.2 \times 10^{-19}$  cm<sup>2</sup> W<sup>-1</sup> and  $\tau_\kappa = 70$  fs in equation (3), respectively. The remaining describes the plasma defocusing due to the electron density  $n_e$ , and the multiphoton absorption with the coefficient of  $\beta^{(K)} = 3.1 \times 10^{-98}$  cm<sup>13</sup> W<sup>-7</sup> and the number of photons  $K = 8$ . In addition, the critical plasma density is  $n_c = 1.7 \times 10^{21}$  cm<sup>-3</sup>, and the initial neutral atom density is  $n_{\text{at}} = 5.4 \times 10^{18}$  cm<sup>-3</sup> in equation (4).

## 3. Results and discussion

In this section, we analyze numerically the impacts of the delayed Kerr nonlinearity on the annular Gaussian filaments nearby the characteristic time of the molecular rotational response. The role of the Raman response in the propagation dynamics of annular Gaussian filaments is also discussed.

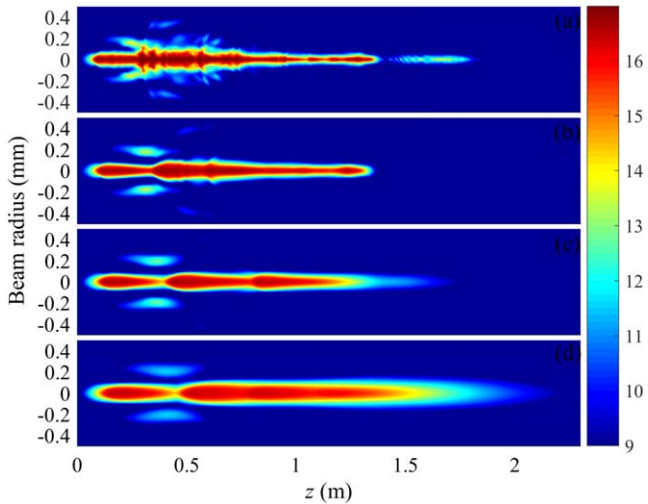


**Figure 1.** The spatial plasma density (in units of  $\text{cm}^{-3}$ ) distribution on a logarithmic scale with the propagation distance  $z$  for Gaussian beam. The contributions of the instantaneous Kerr nonlinearity and the delayed Kerr nonlinearity are (a) (1, 0); (b) (1/2, 1/2); (c) (1/4, 3/4); (d) (0, 1). The input pulse energy, the pulse duration and the width are  $E_{\text{in}} = 3 \text{ mJ}$ ,  $\tau_0 = 60 \text{ fs}$  and  $w_0 = 1 \text{ mm}$ , respectively. The spatial chirp is  $C = 11 \text{ mm}^{-1}$ , and the focal distance of concave is  $f = -8 \text{ m}$ .

### 3.1. Influence of the delayed Kerr nonlinearity on the optical filaments

First, an annular Gaussian beam is focused by a set of lens, which is composed of an axicon and plano-concave lens. When the beam radius is zero ( $r_0 = 0$ ), which is in fact the conventional Gaussian beam, the spatial distribution of the plasma density is shown in figure 1. Figures 1(a)–(d) denote that the contributions of the instantaneous Kerr nonlinearity and the delayed Kerr nonlinearity are (1, 0), (1/2, 1/2), (1/4, 3/4), and (0, 1), respectively. It is clear to see that the plasma string gets more uniform and stable with increasing the delayed Kerr nonlinearity. Although we use the particular focusing geometry optical system, this result is qualitatively consistent with the [28]. However, when the beam radius is not equal to zero ( $r_0 \neq 0$ ), the incident pulse is an annular Gaussian beam. Next, we mainly discuss the influences of the delayed Kerr nonlinearity on the annular Gaussian filaments for the given different initial pulse lengths. The parameters are chosen as follows,  $E_{\text{in}} = 5 \text{ mJ}$ ,  $w_0 = 1 \text{ mm}$  and  $r_0 = 3 \text{ mm}$  are the energy of the input pulse, the width and the radius of annular Gaussian beam, respectively, which are consistent with the [32]. In addition, we have discussed in detail the effects of the different geometry focusing (i.e.  $C$  and  $f$ ) on the characteristics of ring-Gaussian filaments in the [33]. Here, the spatial chirp  $C = 11 \text{ mm}^{-1}$  (the corresponding the cone angle of the axicon lens,  $\alpha = C/k_0(n - 1) = 0.178^\circ$ , by assuming  $n = 1.45$ ) and the focal distance of concave  $f = -8 \text{ m}$  are tuned to remain constant.

Figure 2(a) gives the evolution of the peak plasma density with different initial pulse duration  $\tau_0$  for the annular Gaussian beam. The black and the blue lines, respectively, denote that the nonlinear self-focusing only involves the

instantaneous contribution and includes the instantaneous and retard contributions. The corresponding energy loss as a function of the propagation distance  $z$  is shown in figure 2(b). In figure 2(a), the delayed Kerr nonlinearity acts scarcely to the characteristics of filamentation for the short pulse (see  $\tau_0 = 40 \text{ fs}$  in figure 2(a)). That is the reason why the delayed Kerr nonlinearity in our previous work [32, 33] is neglected. In the presence of the delayed Kerr nonlinearity, the filament onset distance is advanced and the filament length is extended, simultaneously, the peak plasma density appears great oscillations that makes the filament become unstable and nonuniform at the initial pulse duration  $\tau_0 = 60 \text{ fs}$ . Furthermore, at the other values of the initial pulse duration (such as  $\tau_0 = 65, 70, 80$  and  $85 \text{ fs}$ ), the similar phenomenon are observed. Figure 2(c) presents quantitatively the onset distance (solid diamond and circle lines) and the length (dashed open diamond and circle lines) of the filament with different initial pulse duration  $\tau_0$  in the case of pure instantaneous nonlinearity (black lines) and the presence of delayed Kerr nonlinearity (blue lines) for the annular Gaussian beam. On the one hand, it is also easy to see that the blue solid circle line is always lower than the black solid diamond line at a fixed pulse duration. This means that the onset distance is advanced by the presence of delayed Kerr nonlinearity, whereas, as the pulse duration increases, the onset distances are delayed for both the pure instantaneous nonlinearity and the presence of delayed Kerr nonlinearity due to the reduction of input power (see the inset), which is similar to the result of the Gaussian filament [35]. On the other hand, the filament length, which is defined as from the onset distance to the value of the peak plasma density less than  $10^{14} \text{ cm}^{-3}$  at the last beam collapse, in the presence of delayed Kerr nonlinearity (blue dashed open circle line) is always larger than that in the case of pure instantaneous nonlinearity (black dashed open diamond line) at a fixed pulse duration, which means that the length of the filament is extended by the presence of delayed Kerr nonlinearity. When the initial pulse durations ( $\tau_0 = 100 \text{ fs}$ ) is far from the characteristic time, the effect of the delayed Kerr nonlinearity is weakened by the reduction of the initial power on account of the increasing pulse duration. Therefore, the characteristics of optical filament are strongly influenced by the delayed Kerr nonlinearity near the characteristic time of the molecular rotational response ( $\tau_k = 70 \text{ fs}$ ). These results are slightly different from the conventional Gaussian filament in [28].

The delayed Kerr nonlinearity results in the extension of the annular Gaussian filaments nearby the characteristic time of the molecular rotational response, which can also be seen from the evolution of the total energy loss (see figure 2(b)). It is obvious that, near the characteristic time  $\tau_k$ , the total energy loss speed of optical filament in the presence of the delayed Kerr nonlinearity is slower than in the case of the pure instantaneous Kerr nonlinearity. For example, at the initial pulse duration  $\tau_0 = 65 \text{ fs}$ , in the case of pure instantaneous nonlinearity, the pulse energy decreases of  $\Delta E/E_{\text{in}} \approx 9\%$  over about 3.1 m, while in the presence of the delayed Kerr nonlinearity, the energy drops of  $\Delta E/E_{\text{in}} \approx 8.2\%$  over about 4.9 m. The slow energy loss leads to the extension of the

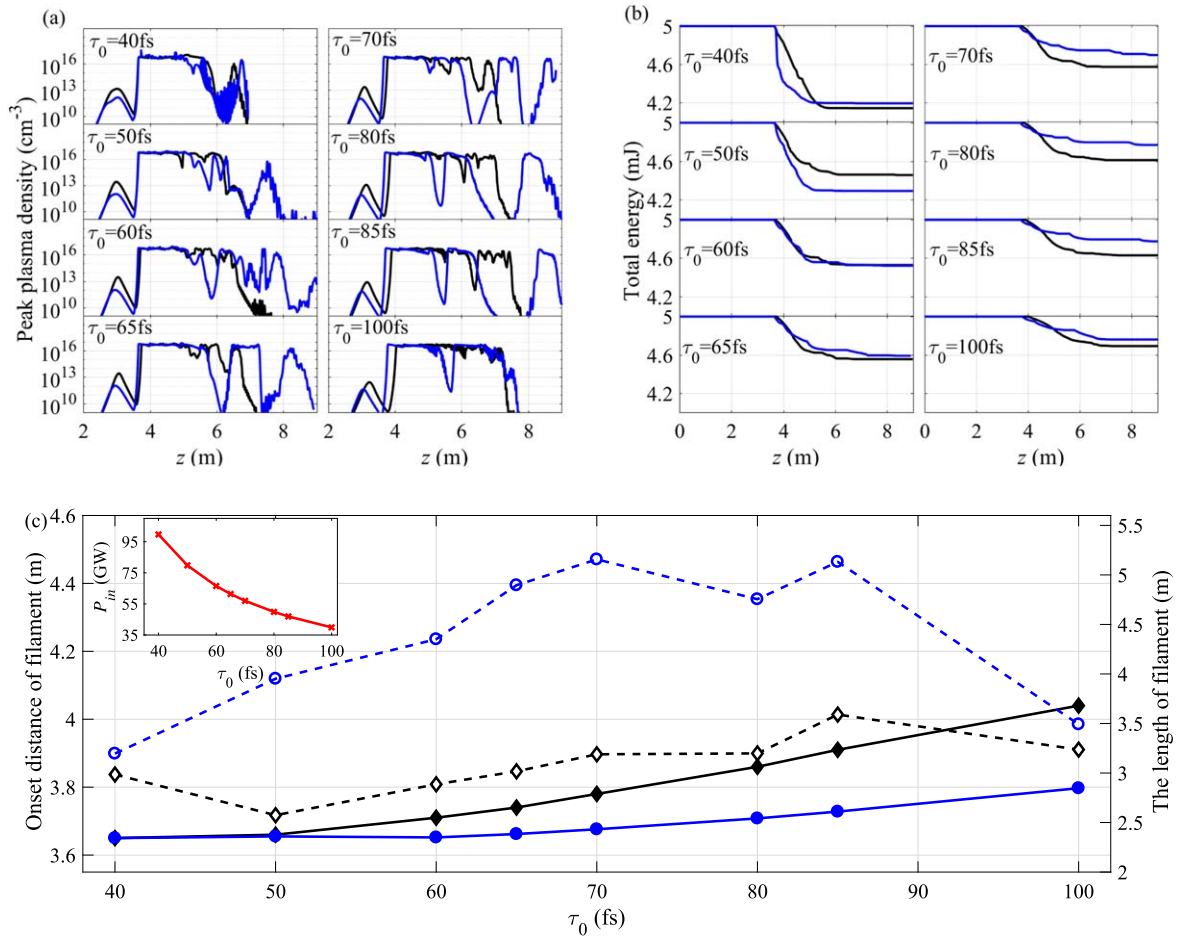


**Figure 2.** (a) The peak plasma density; (b) the energy loss as a function of the propagation distance  $z$  with different initial pulse duration  $\tau_0$  in the case of pure instantaneous nonlinearity (black lines) and the presence of delayed Kerr nonlinearity (blue lines) for annular Gaussian beam. (c) The onset distance (solid diamond and circle lines) and the length (dashed open diamond and circle lines) of filament with different initial pulse duration  $\tau_0$  in the case of pure instantaneous nonlinearity (black lines) and the presence of delayed Kerr nonlinearity (blue lines) for annular Gaussian beam. In the inset, the input power is as a function of initial pulse duration  $\tau_0$ . The input energy is  $E_{in} = 5$  mJ, the spatial chirp is  $C = 11$  mm<sup>-1</sup>, and the focal distance of concave is  $f = -8$  m.

filament (see blue solid line in figures 2(a) and (b)). A further understanding of the role of the delayed Kerr effect needs to be analyzed from the propagation dynamics of the optical filament.

### 3.2. The propagation dynamics of the annular Gaussian filaments

Here, the characteristics of Raman response are investigated from the spatial distribution and the temporal dynamics behavior of annular Gaussian filaments. Figures 3(a) and (b) present the distribution of the spatial plasma density on a logarithmic scale and the fluence ( $F(r, z) = \int_{-\infty}^{\infty} |A(r, t, z)|^2 dt$ ) with the propagation distance  $z$  in the case of pure instantaneous nonlinearity (top) and the presence of delayed Kerr nonlinearity (bottom) at the initial pulse duration  $\tau_0 = 60$  fs. The delayed Kerr nonlinearity increases the length of the plasma string (see figure 3(a)), which can be explained from the spatial distribution of the fluence. From figure 3(b), we can see that, before the formation of the optical filament, the fluence with the delayed Kerr nonlinearity is less than that of the pure instantaneous

nonlinearity. For example, at the propagation distance  $z = 3.075$  m, the maximal fluence,  $F_{max} = 0.99 \times 10^3$  mJ cm<sup>-2</sup> in the presence of delayed Kerr nonlinearity and  $F_{max} = 1.57 \times 10^3$  mJ cm<sup>-2</sup> in the case of pure instantaneous nonlinearity. This is because that the presence of delayed Kerr nonlinearity declines the self-focusing effect and suppresses the increase of the fluence when the beam intensity and the plasma density are low. Therefore, the fluence with the delayed Kerr nonlinearity is less than that of the pure instantaneous nonlinearity. Meanwhile, after the formation of the optical filament, the optical filament intensity reaches the clamping intensity and the nonlinear self-focusing is related to  $N_{Kerr}$ , which is proportional to the filament intensity (see equation (3)). As shown in figure 3(b), at the propagation distance  $z = 3.794$  m, the maximal fluence,  $F_{max} = 3.23 \times 10^3$  mJ cm<sup>-2</sup> in the presence of delayed Kerr nonlinearity is larger than  $F_{max} = 1.73 \times 10^3$  mJ cm<sup>-2</sup> in the case of pure instantaneous nonlinearity. Hence, the delayed Kerr nonlinearity promotes greatly the increase of the fluence, which exceeds the case of the pure instantaneous nonlinearity. At the same time, the large fluence rises rapidly the plasma density at the threshold of the filament,

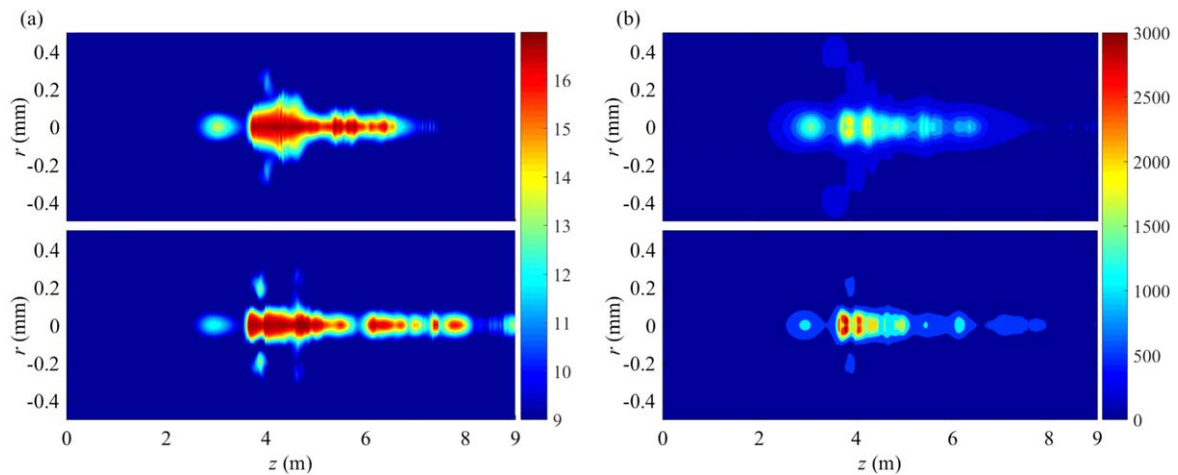


**Figure 3.** The distribution of the spatial plasma density (a) (in units of  $\text{cm}^{-3}$ ) on a logarithmic scale and the fluence (b) (in units of  $\text{mJ cm}^{-2}$ ) with the propagation distance  $z$  in the case of pure instantaneous nonlinearity (top) and the presence of delayed Kerr nonlinearity (bottom) at the initial pulse duration  $\tau_0 = 60$  fs for annular Gaussian beam. The parameters  $E$ ,  $C$  and  $f$  are same as in figure 2.

which induces an abrupt loss of the energy (see in figure 2(b)). As the propagation of the optical filament, the abrupt energy loss reduces quickly the plasma density and makes it appear a dip. At the moment, the beam power (about 60 GW) is still higher than the critical power that results in the refocusing of the pulse. It means that the peak plasma density occurs the great oscillations that makes the filament become unstable and nonuniform (see in figure 2(a)). Then, the energy loss also becomes slowing down. The total loss of energy with the delayed Kerr nonlinearity is less than the case of that pure instantaneous nonlinearity near the characteristic time in figure 2(b), where the blue lines are above the black lines after the cross. Eventually, the optical filament is extended in the presence of the delayed Kerr nonlinearity.

In order to adequately understand the influences of delayed Kerr nonlinearity on the annular Gaussian filament, we analyze the temporal behavior of annular Gaussian filaments at the input pulse duration  $\tau_0 = 60$  fs. Figure 4(a) shows the temporal distribution of the on-axis intensity in the case of pure instantaneous nonlinearity (top) and the presence of delayed Kerr nonlinearity (bottom). It is easy to see that the delayed Kerr nonlinearity affects strongly the distribution of the intensity before and after the formation of the optical filaments. The temporal distributions of the on-axis intensity at different propagation distances  $z$  are shown in figure 4(b). The black and the blue lines, respectively, denote that the nonlinear self-focusing only involves the instantaneous contribution and includes the instantaneous and retard contributions. As described in [32], for the case of purely instantaneous Kerr nonlinearity before the formation of the optical filament (see the black lines in figure 4(b)), two peaks appear symmetrically due to the pulse splitting. Then the two peaks are delayed gradually in time when the intensity of the two peaks decreases. During laser pulse propagation, another splitting event occurs, while the presence of the delayed Kerr nonlinearity makes the pulse no longer split symmetrically and declines the intensity of the laser pulse. Moreover, the intensity of the back of the pulse decreases much faster than

that of the front of the pulse at a propagation distance between  $z = 2.95\text{--}3.4$  m, and thereby, a leading edge of the pulse is formed. As the propagation of laser pulse, the self-focusing effect of the pulse front is weakened and the plasmas are partly turned off. Then, the refocusing of the trailing edge is aroused, which makes the energy refuel the center of the pulse. So the central intensity rises rapidly between  $z = 3.4\text{--}3.6$  m, which results in the advancement of the onset distance in the presence of the delayed Kerr nonlinearity. Furthermore, comparing blue line with black line in figure 4(b)), it is easy to see that the delayed Kerr nonlinearity causes the self-focusing for the trailing edge of the pulse to be significantly enhanced after the formation of the optical filament ( $z > 3.65$  m), and the refocusing cycles in the case of the presence of the delayed Kerr nonlinearity is more than in the case of the pure instantaneous nonlinearity. Additionally, the refocusing processes also lead to the beam in the trailing part oscillation. At last, the annular Gaussian filament is extended as shown in the bottom of figures 3(a) and 4(a). Note that, although the delayed Kerr nonlinearity makes the filament length be extended for both an annular Gaussian beam and a Gaussian beam [28], the nonlinear dynamics mechanism of the two laser pulses is completely different. The initial transverse distribution of the annular Gaussian beam led to the pulse splitting and the redistribution of the pulse energy of the annular Gaussian beam, which was specifically analyzed in our previous work [32]. Consequently, when adding the delayed Kerr nonlinearity, the different dynamics mechanism results in the different propagation characteristics (the onset distance and uniformity of filaments) between the two laser pulses.

In addition, the spectral intensity at some propagation distance corresponding to figure 4(b) are shown in figure 4(c), and the red dot line denotes the initial spectrum. We can see that the spectra are extended with increasing propagation distance. Particularly, the widths of spectra start to increase evidently as soon as the filament forms ( $z > 3.65$  m). Moreover, the delayed Kerr nonlinearity enhances the spectra towards the

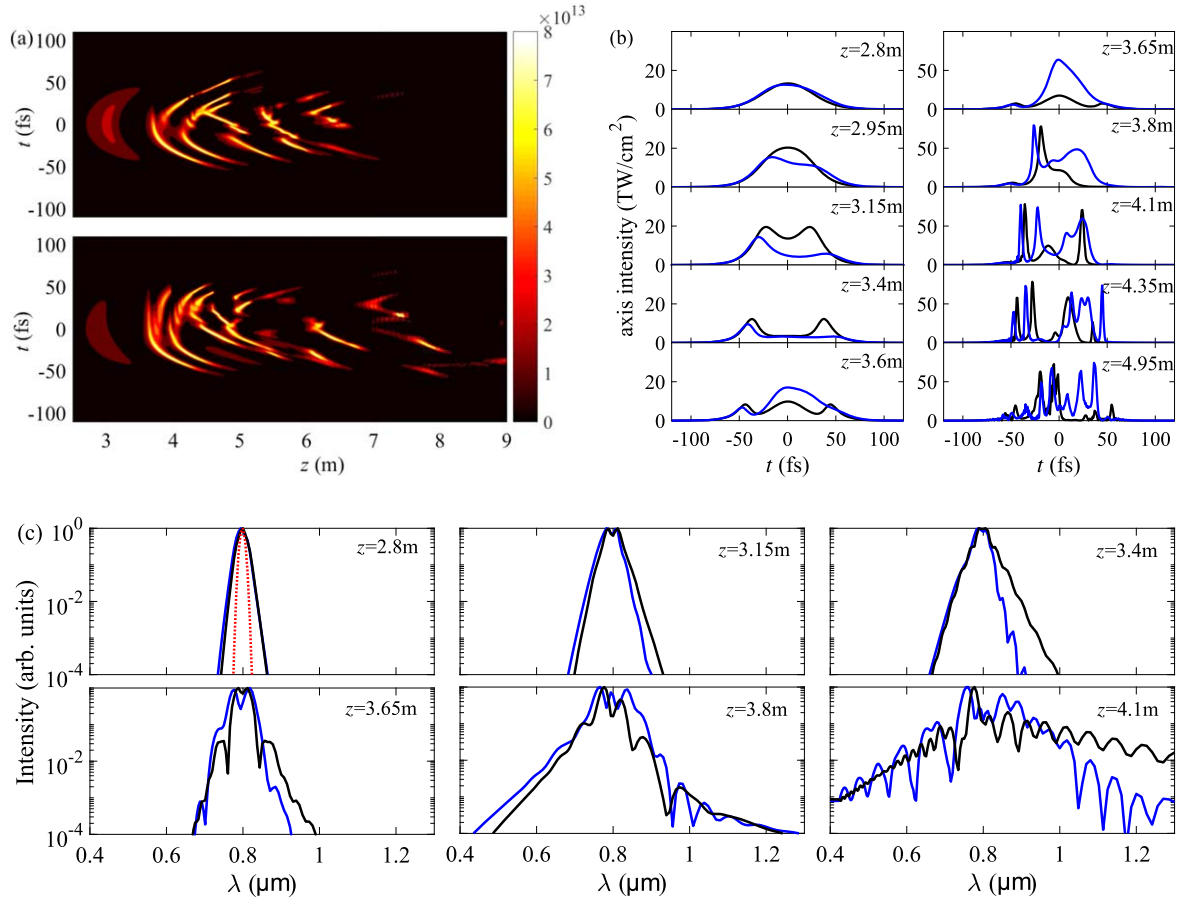


**Figure 4.** (a) The temporal distribution of the on-axis intensity (in units of  $\text{W cm}^{-2}$ ) with the propagation distance  $z$  in the case of pure instantaneous nonlinearity (top) and the presence of delayed Kerr nonlinearity (bottom) at the initial pulse duration  $\tau_0 = 60$  fs for annular Gaussian beam. (b) The temporal distribution of the on-axis intensity and (c) the spectral profiles at some propagation distance  $z$  and the red dot line denotes the initial spectrum. The black and blue lines and other parameters are same as in figure 2.

blue side. This Raman blue shifting effect is similar with the case of the Gaussian filament [27, 28]. During the propagation of the filament, the spectra are distorted and oscillated, which are caused by constructive/destructive interference between different temporal peaks emerging in the pulse profile. Simultaneously, the strong modulations of the spectra also lead to a dramatic distortion of the pulse time profile.

#### 4. Conclusions

We have theoretically investigated the influences of the delayed Kerr nonlinearity on the propagation of femtosecond annular Gaussian filaments in air. When the pulse duration is fixed, the filament onset distance is advanced in the presence of delayed Kerr nonlinearity compared with the case of pure instantaneous Kerr nonlinearity. Simultaneously, whether or not the presence of the delayed Kerr nonlinearity, the onset distances are delayed with increasing the pulse duration. In the presence of delayed Kerr nonlinearity, nearby the characteristic time of the molecular rotational respond ( $\tau_k = 70$  fs), the length of the filament is extended obviously, and the peak plasma density appears the great oscillations that makes the filament become unstable and nonuniform. Moreover, the

delayed Kerr nonlinearity also influences strongly the propagation dynamics of the annular Gaussian filaments. The fluence is redistributed in the presence of the delayed Kerr effect, which leads to the reduction of the total energy loss speed and extends the length of the optical filament. In addition, through the temporal dynamics of annular Gaussian filaments, we have also discovered that the presence of the delayed Kerr effect makes the pulse split asymmetrically before the formation of optical filament, which causes the onset distance of filament to be advanced. Furthermore, after the formation of the optical filament, the contribution of the delayed Kerr nonlinearity enhances the self-focusing of the trailing edge of the pulse and causes the filament propagation to present the multiple refocusing cycles. Thereby, the annular Gaussian filament is extended. In short, the study of the effects of the delayed Kerr nonlinearity for annular Gaussian filaments is a great significance to understand deeply the long-distance transmission characteristics of the annular Gaussian filaments.

#### Acknowledgments

This work is supported by the National Natural Science Foundation of China (Grant Nos. 11674034, 11775030, 11725417,

11575027, 11822401), the Natural Science Foundation of Shanxi Province, China (Grant No. 201601D021019), the Scientific and Technological Innovation Programs of Higher Education Institutions in Shanxi (Grant No. 2017163), Foundation of the Outstanding Young Scholars of Shanxi Province, China (Grant No. 201801D211006), the Fund for Shanxi '1331 Project' Key Innovative Research Team (1331KIRT), the NSAF (No. U1730449), the Science Challenge Project (Grant No. TZ2018005) and the National Key R&D Program of China (Grant No. 2018YFB0504400).

## ORCID iDs

Junping Lan  <https://orcid.org/0000-0001-9302-0518>

Yuan Liu  <https://orcid.org/0000-0002-4762-0325>

Zhifang Feng  <https://orcid.org/0000-0002-8647-0585>

## References

- [1] Wolf J-P 2018 *Rep. Prog. Phys.* **81** 026001
- [2] Couairon A and Mysyrowicz A 2007 *Phys. Rep.* **441** 47
- [3] Berg L, Skupin S, Nuter R, Kasparian J and Wolf J-P 2007 *Rep. Prog. Phys.* **70** 1633
- [4] Chin S L, Hosseini S A, Liu W, Luo Q, Thberge F, Akzbek N, Becker A, Kandidov V P, Kosareva O G and Schroeder H 2005 *Can. J. Phys.* **83** 863
- [5] Stelmaszczyk K, Rohwetter P, Méjean G, Yu J, Salmon E, Kasparian J, Ackermann R, Wolf J-P and Wste L 2004 *Appl. Phys. Lett.* **85** 3977
- [6] Xu H L, Méjean G, Liu W, Kamali Y, Daigle J F, Azarm A, Simard P T, Mathieu P, Roy G, Simard J R and Chin S L 2007 *Appl. Phys. B* **87** 151
- [7] Chin S L and Miyazaki K 1999 *Japan. J. Appl. Phys.* **38** 2011
- [8] Rodriguez M et al 2002 *Opt. Lett.* **27** 772
- [9] Méjean G et al 2006 *Appl. Phys. Lett.* **88** 021101
- [10] Xu H L, Daigle J F, Luo Q and Chin S L 2006 *Appl. Phys. B* **82** 655
- [11] Luo Q, Xu H L, Hosseini S A, Daigle J-F, Théberge F, Sharifi M and Chin S L 2006 *Appl. Phys. B* **82** 105
- [12] Kasparian J et al 2003 *Science* **301** 61
- [13] Sharma A, Misra S, Mishra S K and Kourakis I 2013 *Phys. Rev. E* **87** 063111
- [14] Hussain S, Singh M, Singh R K and Sharma R P 2014 *Europhys. Lett.* **107** 65002
- [15] Panagiotopoulos P, Papazoglou D G, Couairon A and Tzortzakis S 2013 *Nat. Commun.* **4** 2622
- [16] Arnold C L et al 2015 *J. Phys. B: At. Mol. Opt. Phys.* **48** 094006
- [17] Kaya G, Kaya N, Sayrac M, Boran Y, Strohaber J, Kolomenskii A A, Amani M and Schuessler H A 2016 *AIP Adv.* **6** 035001
- [18] Zhang Y-Q, Ji X-L, Li X-Q, Li Q and Yu H 2017 *Opt. Express* **25** 21329
- [19] Mills M, Heinrich M, Kolesik M and Christodoulides D 2015 *J. Phys. B: At. Mol. Opt. Phys.* **48** 094014
- [20] Geints Y E and Zemlyanov A A 2017 *J. Opt.* **19** 105502
- [21] York A G, Milchberg H M, Palastro J P and Antonsen T M 2008 *Phys. Rev. Lett.* **100** 195001
- [22] Paez-Lopez R, Ruiz U, Arrizon V and Ramos-Garcia R 2016 *Opt. Lett.* **41** 4138
- [23] Shvedov V G, Rode A V, Izdebskaya Y V, Desyatnikov A S, Krolikowski W and Kivshar Y S 2010 *Phys. Rev. Lett.* **105** 118103
- [24] Ripoche J-F, Grillon G, Prade B, Franco M, Nibbering E, Lange R and Mysyrowicz A 1997 *Opt. Commun.* **135** 310
- [25] Nibbering E T J, Grillon G, Franco M A, Prade B S and Mysyrowicz A 1997 *J. Opt. Soc. Am. B* **14** 650
- [26] Varma S, Chen Y-H and Milchberg H M 2008 *Phys. Rev. Lett.* **101** 205001
- [27] Chiron A, Lamouroux B, Lange R, Ripoche J-F, Franco M, Prade B, Bonnaud G, Riazuelo G and Mysyrowicz A 1999 *Eur. Phys. J. D* **6** 383
- [28] Nurhuda M and Van-Groesen E 2005 *Phys. Rev. E* **71** 066502
- [29] Wang L, Ma C-L, Qi X-X and Lin W-B 2015 *Eur. Phys. J. D* **69** 72
- [30] Couairon A and Bergé L 2000 *Phys. Plasmas* **7** 193
- [31] Chin S L, Aközbek N, Proulx A, Petit S and Bowden C M 2001 *Opt. Commun.* **188** 181
- [32] Feng Z F, Li W, Yu C X, Liu X, Liu J and Fu L B 2015 *Phys. Rev. A* **91** 033839
- [33] Feng Z F, Li W, Yu C X, Liu X, Liu Y, Liu J and Fu L B 2016 *Opt. Express* **24** 6381
- [34] Abdollahpour D, Panagiotopoulos P, Turconi M, Jedrkiewicz O, Faccio D, Trapani P, Di, Couairon A, Papazoglou D G and Tzortzakis S 2009 *Opt. Express* **17** 5052
- [35] Couairon A 2003 *Eur. Phys. J. D* **27** 159